

# Palmprint Identification Based on Fusion Of KWT and DWT at Matching Score Level

K. P. Shashikala<sup>1</sup> and K. B. Raja<sup>2</sup>

**Abstract:** Palmprint is a physiological biometric trait and is efficient in identifying a person. In this paper we propose Palmprint Identification based on fusion of KWT and DWT at matching Score level (PIFKDM). The palmprint image is preprocessed to generate histogram equalized ROI. The KWT and DWT are applied on preprocessed image. The KWT coefficients and LL band of DWT are considered as features. The EER and TSR values are computed using KWT and DWT features. The EER and TSR values of KWT and DWT are fused using Log Transformation to get better performance. It is observed that the values of performance parameters are better in the case of proposed algorithm compared to existing algorithms.

**Index Terms** — Palmprint, Fusion, KWT, DWT, ED, EER, TSR

## 1 INTRODUCTION

Automatic human Identification based on Biometrics is becoming a compelling need in today's globally connected society. It is a technique for measuring the unique human characteristics for identification or verification. Further it is being used extensively in access control and in surveillance applications instead of PIN, passwords, ID Cards, RF ID tagsetc. Biometrics is giving way to a new technology called e-passport around the world which is a combination of Biometrics, Smart card and RF technology. Biometrics can be physiological or behavioral. The physiological biometric modalities are fingerprints, palmprints, face iris, ear, etc. Behavioral biometric modalities are voice, gait, signature, typing style etc. Any biometric modality must be universal, unique, permanent, collectable and acceptable to be practically implemented. Palmprints satisfy all these characteristics. Palmprint is rich with substantial and discriminating information. Unique low resolution features like principle lines, wrinkles and high resolution, Texture features such as minutiae points, ridges, bifurcations etc. These features can be fused to obtain a more robust system. The requirement of a biometric system is low cost, high accuracy, illumination invariance, fast feature extraction, fast matching speeds and lesser memory requirement.

A typical recognition system consists of a database, preprocessing, feature extraction and matching unit.

(i) *Database:* Poly U palmprint database is used in our paper.

(ii) *Preprocessing:* It involves some algorithm to extract a Region

(iii) *Feature extraction :* Algorithms such as, Principle Component Analysis, Linear Discriminant Analysis, Independent Component Analysis etc. can be used to produce spatial domain features. These features can be further coupled with various types of transforms such as FFT, DCT, DWT and various other complex wavelets.

Unique Identification Authority of India, UIDAI is implementing Aadhar scheme which aims to provide a unique ID number to every Indian citizen. The multimodal biometric information from each citizen consisting of face, ten fingers and iris is used to generate a random ID number which is not dependent on class, creed, religion and geography, hoping to provide a secure and accurate access to the 1.2 billion people of India in all walks of life.

*Contribution:* In this paper KWT and DWT are used to extract features and compute TSR and EER performance parameters. The performance parameters are fused at matching level using Log transformation to improve performance of the algorithm.

## 2. LITERATURE SURVEY

Kekre et al., [1] proposed a Hybrid wavelet transform on multispectral palmprints, which is a Kronecker product of any two existing wavelet transforms such as Walsh and Kekre Wavelet Transform. The hybrid wavelet has the advantages of multi-resolution analysis. The Hybrid wavelet coefficients are compacted and fusion of the multispectral image features by OR and AND techniques is done to find the best technique. Xingpeng Xu et al., [2] use multispectral palmprint images which ensure better accuracy. Multispectral images of NIR, Red, Blue and Green are represented by Quaternion Matrix. QPCA and QDWT are applied separately to data and test images. Euclidean distance is found for the two QPCA and QDWT features of the test and data base images. The final decision is taken based on the fusion of QPCA and QDWT distances. Wei Li et al., [3] proposed 2D and 3D palm features consisting of shape, principle lines and textures aligned and fused by ICP method and matching rules based on the matching dis-

- 
- K. P. Shashikala, Ph.D Registration Number: PP ECE 022, Subject of Registration: Electronics and Communication Engineering, Rayalseema University, Kurnool, AP, India Email: kp.shashikala@gmail.com
  - Raja K B, Department of ECE, University Visveswaraya College of Engineering, Bangalore University, Bangalore, India, Email: rajakb429@gmail.com

tance. Wei li et al., [4] proposed a refined alignment for the extraction of ROI. An iterative closest point method between the images is used on the palm features for matching. Kumar et al., [5] proposed a low cost contactless palm image acquisition system. Band limited phase only correlation (BLPOC) is used for comparing images. The ROI of the image is quantized and the phase angle coefficients are used for matching. Ruiqiong Shi and Dongmei Sun [6] proposed a biometric template which is used as a secret key from palmprint images using 2D Gabor filters. Eryun Liu et al., [7] proposed a fine to course matching strategy involving minutiae clustering and minutiae match propagation for Latent palmprint matching. Feng Yue et al., [8] put forth two hashing based techniques for fast palmprint Identification. The first method is based on Orientation Pattern (OP) hashing and the second method is based on Principle Orientation Pattern (POP) hashing. Struc and Pavesic [9] applied various normalization techniques on the feature vectors obtained from palm images with the help of PCA. Guassianization was found to be most effective. Lin Lin Shen et al., [10] encode the relationship between the magnitude of wavelet response to the central pixel with respect to nearest neighbors by convolving Gabor wavelet with palmprint and Local Binary Pattern (LBP). Hardware implementation is done by OMAP 3530 processor. Gandehari and Avanthipur [11] found the local histogram of oriented gradients of palmprints at each level of Gaussian pyramid, extracting short and high contrast lines and applied tree based matching. Chau [12] proposed fusion of matching scores of principle lines and Locality Preserving Projections (LPP). Gayathri and Ramamurthy [13] use Gabor wavelet to extract and fuse multiple features such as contrast, correlation, energy and homogeneity. Matching is done by nearest neighbor classifier. Lin Zhang et al., [14] represent the changing palmprint texture in changing images of the same palmprint by fragile bits. These fragile bits are mapped by Binary Orientation Co Occurrence Vector (BOCV) and masked while calculating Hamming Distance. Dakshina et al., [15] proposed Multispectral palm images of the same person are to be fused by wavelet transform and convolved with Gabor Wavelet Transform to obtain features. Dimensionality reduction is done by Ant Colony Optimization (ACO). SVM is used for training and matching. Hanmandal et al., [16] proposed four different approaches and compared the feature extraction by fuzzy logic, Multiscale Wavelet, Sigmoid and Local Binary Pattern (LBP). Matching by Euclidean Distance and SVM was done. Capelli et al., [17] employ high resolution palm image for minutiae feature extraction. Local matching strategy is employed for matching. Huan Zhang [18] collects fractal images (ROI) from the users reducing computation time. Fractal coding is used for matching. Vinayak Baradi [19] proposed initial transform of two dimensional image and next step transformations to generate complex planes for feature extraction. The transforms used are Walsh, DCT, Hartley, Kekre and Kekre Wavelet Transforms. Both Unimodal and Multimodal fusion consisting of fingerprint, palmprint, Iris and finger knuckle prints are tested. Kekre et al., [20] propose a novel Kekre's wavelet Transform which is generated from Kekre's Transform. This is a faster Transform which can be used for various image pro-

cessing applications. In this paper they have implemented Steganography. Kekre et al., [21] use Kekre wavelet for feature Extraction. The relative energy entropy of the decomposed images and Euclidean distance is used for matching. Haifeng Sang et al., [22] use skin color thresholding and hand valley detection for extracting palmprint ROI. Local Binary Pattern (LBP) is applied to obtain features. Chi-Square Statistics used for classification. Jingyuguo et al., [23] proposed feature extraction by Entropy Map and 2DPCA. The effect of illumination and Dimensionality are reduced. Nearest neighbor Classification is used. Khalifa et al., [24] proposed feature extraction by Wavelet, Gabor filter and Co-occurrence matrix and SVM for matching.

**3. PROPOSED PIFKDM MODEL:**

In this section definitions of performance parameters and block diagram of proposed model are discussed.

**3.1.1 False Acceptance Rate (FAR)** it is the measure of the percentage of falsely accepted palmprints. It is the ratio of the number of invalid palmprints accepted to the total number of palmprints present in outside database as given in equation 1.

$$FAR = \frac{\text{No of invalid palmprint accepted}}{\text{No of palmprint in outside the database}} \dots\dots(1)$$

**3.1.2 False Rejection Rate (FRR):** It is the ratio of number of valid palmprints rejected to the total number of persons in the database as given in equation 2.

$$FRR = \frac{\text{No of valid palmprint rejected}}{\text{No of palmprint in the database}} \dots\dots\dots(2)$$

**3.1.3 Equal Error Rate (EER)** It is the rate at which accept and reject rates are equal. It is obtained from the plot of FAR and FRR with respect to threshold as given in equation 3.

$$EER = FAR = FRR \dots\dots\dots(3)$$

**3.1.4 Total Success Rate (TSR)** gives the number of persons correctly matched out of the total number of persons present in the database as given in equation 4.

$$TSR = \frac{\text{No of test images correctly matched}}{\text{Total no of Persons in database}} \dots\dots\dots(4)$$

**3.2 Proposed Block diagram of PIFKDM:**

The block diagram of the proposed model is as shown in the figure 1. The features are extracted using KWT and DWT. The Euclidean Distance is used to compare features of test images with features of images in the database. The matching scores are fused at matching level. The performance parameter values are improved since performance parameters scores using KWT and DWT are fused at matching level using Log transformation.

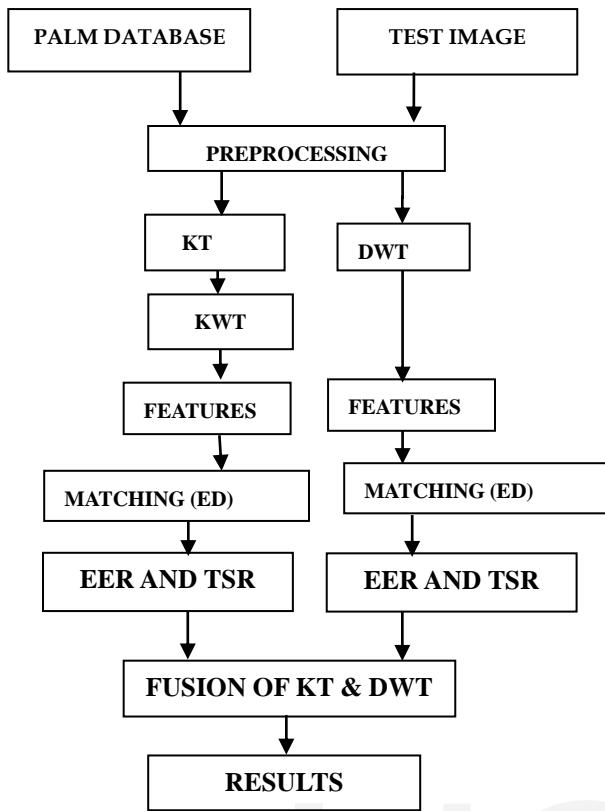


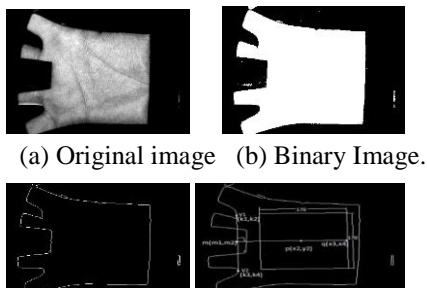
Figure 1 Model of PIFKDM

3.2.1 DataBase:

The Poly U database consists of palmprint images of 386 persons with 20 images per person. Every eighteenth image in the database is considered as test image. The different combinations of number of persons inside and outside database is considered in the range of 20; 100, 40:80, 60:60, 80:40 and 100:20 to compute FRR, TSR, FAR and EER for both the KWT and DWT respectively.

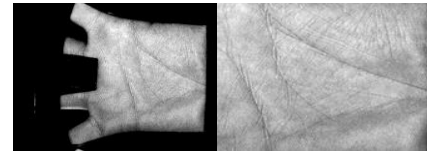
3.2.2 Preprocessing

The original palmprint image of size 384x284 is converted into binary image to obtain proper edges. The Canny edge detection is applied on the binary image to get boundary of the palmprint. The ROI is obtained using linear equations and normalization. The image is cropped to 170x170. The Histogram Equalization is applied on the ROI for contrast enhancement. The image is again resized to 64 X 64. The original image, Binary image, Edge detected image, ROI Detection Scheme, Normalized palmprint, and ROI and Histogram Equalized ROI are shown in Figures 2.



(a) Original image (b) Binary Image.

(c) Edge detected image (d) ROI detection scheme



(e) Normalized image (f) Region of Interest



(g) Histogram Equalized ROI

Figure 2: Preprocessing of Palmprint.

The valley points  $v1 (k1, k2)$  and  $v2 (k3, k4)$  are located by comparing the distances between the midpoint of the image and the borders of the palm as shown in Figure 4. The midpoint  $m(m1, m2)$  of the line joining  $v1$  and  $v2$  is found using Equation (5) and (6).

$$m1 = \frac{(k1 + k3)}{2} \dots\dots\dots (5)$$

$$m2 = \frac{(k2 + k4)}{2} \dots\dots\dots (6)$$

Slope of the perpendicular bisector of  $v1v2$  is then found out using Equation (7).

$$s = \frac{-(k3 - k1)}{(k4 - k2)} \dots\dots\dots (7)$$

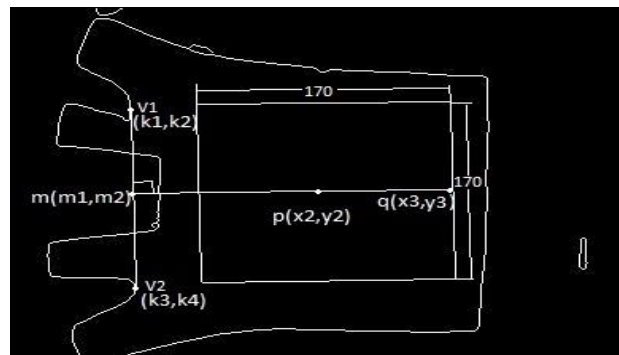


Figure3: ROI Detection

The point's  $p(x_2, y_2)$  and  $q(x_3, y_3)$  are obtained using the Equation (8).

$$(x_2 - m_1) * s = (y_2 - m_2) \dots \dots (8)$$

The point's  $p$  and  $q$  lie on the same line but at different distances.



Figure4: Angle Estimation

The angle  $\alpha$  between the two point's  $p$  and  $q$  is used to find the orientation of the palm as shown in Figure 4. The image is rotated by angle  $\alpha$  in order to correct the wrong orientation. The angle is given by Equation (9).

$$\alpha = \tan^{-1} \left( \frac{y_3 - y_1}{x_2 - x_1} \right) \dots \dots \dots (9)$$

**3.2.3 Kekre Transform (KT):**

Kekre transform can be used for easy storage and fast retrieval of images from large databases. The biometric database is very large taking up large memory space and also takes a considerable time for image matching. The KT can be used to store images in the form of feature set which consists of information regarding color, texture or shape. The feature set is of much smaller dimension ensuring fast matching and identification. The KT matrix can be of any size. The central diagonal values of the matrix are one, the upper diagonal values of the matrix are all one and the lower values of the matrix are all zeroes. A generalized KT matrix is as shown in figure 5 and an 8X8 matrix in figure 6.

**Properties of Kekre's Transform**

- (i) The Kekre's transform is a real and orthogonal Transform.  $[K]^T [K] = [I]$   
Where  $[K]^T$  is transpose of  $[K]$  and  $[I]$  is a Diagonal matrix and its elements are given by  $\mu$ .
- (ii) It is a sparse matrix having  $m(m+1)/2$  ones and  $(m-1)(m-2)/2$  zeroes resulting in fast conversion.
- (iii) The Transform of a vector  $f$  is given by:  
 $F = [K]f$
- (iv) The inverse Transform is given by  $f = [K]^T [I]^{-1} F$

1	1	1	.....	1	1
-N+1	1	1	.....	1	1
0	N+2	1	.....	1	1
.	.	.	.....	.	.
0	0	0	.....	1	1
0	0	0	.....	-N+(N-1)	1

Figure 5: NXN Kekre transform matrix

$$k(x, y) = \begin{cases} 1 & , x \leq y \\ -N + (x - 1) & , x = y + 1 \dots \dots \dots (10) \\ 0 & , x > y + 1 \end{cases}$$

1	1	1	1	1	1	1	1
-7	1	1	1	1	1	1	1
0	-6	1	1	1	1	1	1
0	0	-5	1	1	1	1	1
0	0	0	-4	1	1	1	1
0	0	0	0	-3	1	1	1
0	0	0	0	0	-2	1	1
0	0	0	0	0	0	-1	1

Figure 6: 8x8 Kekre Transform matrix

**3.2.4 Kekre Wavelet Transform (KWT)**

Kekre Wavelet Transform is obtained from Kekre Transform. Kekre wavelet matrices of dimensions  $(2N) \times (2N)$ ,  $(3N) \times (3N)$  ...  $(N^2) \times (N^2)$  can be constructed from an  $N \times N$  Kekre Transform matrix. Thus from an 8x8 Kekre matrix, a 16x16, 24x24, ..., 64x64 matrix can be generated. From an  $N \times N$  Kekre matrix an  $M \times M$  Kekre wavelet transform can be generated, so that  $M = N * P$  Where  $P$  ranges between 2 and  $N$  ( $2 \leq p \leq N$ ). In our method we have used a 64x64 Kekre Wavelet Transform.  $M = 64$ ,  $N = 8$ ,  $P = M/N = 8$ . All the columns of 8x8 Kekre Transform matrix are repeated  $P = 8$  times to generate the first eight rows, the remaining  $(P - 1)$  i.e. 56 rows are obtained from the temporary matrix. Each element of the temporary matrix is repeated 8 times to obtain the remaining 56 rows.

**(i) Orthogonal**

The KWT transform matrix  $K$  is orthogonal as  $[K][K]^T = [D]$   
Where  $D$  is the diagonal matrix.

**(ii) Asymmetric**

The Kekre's transform is an upper triangular matrix, it is asymmetric.

**(iii) Non Involutional**

KWT is the inverse transform of itself.

**(iv) Transform on Vector**

The Kekre's Wavelet transform on a column Vector  $f$  is given by  
 $F = [KW] f$   
And inverse is given by  
 $f = [KW]^T [D]^{-1} F$

**(v) Transform on 2D Matrix:**

Kekre's Wavelet transform on 2D matrix  $F$  is given by  $[F] = [KW] [f] [KW]^T$   
**Inverse KWT Transform:**  
Calculate Diagonal matrix  $D$  as,  
 $[D] = [KW] [KW]^T$   
Inverse is calculated as  
 $[f] = [KW]^T [Fij / Dij] [KW]$   
Where  $Dij = Di * Dj$ ;  $1 \leq i \leq N$  and  $1 \leq j \leq N$

**The Temporary Matrix**

Its dimensions are given by the last (P-1) rows and P columns of the 8x8 Kekre Transform matrix which is a 7x8 matrix as shown in the figure 7.

-7	1	1	1	1	1	1	1
0	-6	1	1	1	1	1	1
0	0	-5	1	1	1	1	1
0	0	0	-4	1	1	1	1
0	0	0	0	-3	1	1	1
0	0	0	0	0	-2	1	1
0	0	0	0	0	0	-1	1

**Figure 7: Temporary Matrix T**

**Algorithm used to Obtain KWT Matrix.**

1. Each columns of KT are repeated P=8 times each generating 64 columns.
2. The first row of temporary matrix is [-7,1, 1, 1, 1, 1, 1, 1]. It is used to generate the next 8 rows. The same digits are repeated in every subsequent 8 columns.
3. The second row [0,-6, 1, 1, 1, 1, 1, 1] is used to generate the next 8 rows and 64 columns.
4. This process is continued for all rows of temporary matrix, getting a 64x64 KWT matrix. The first 16 columns and 18 rows of the 64x64Kekre Wavelet Transform Matrix is as seen in Figure 8.

**KWT Features**

The feature vector is obtained using the Expression:  
**[KWT]\*[Image Matrix] [KWT]<sup>T</sup>..... (11)**

**1<sup>st</sup> column of KT**                      **2<sup>nd</sup> column of KT**  
**RepeatedRepeated**  
**P-1 =7 times**                              **P-1 =7 times**

1 1 1 1 1 1 1 1	1 1 1 1 1 1 1 1
-7 -7 -7 -7 -7 -7 -7 -7	1 1 1 1 1 1 1 1
0 0 0 0 0 0 0 0	-6 -6 -6 -6 -6 -6 -6 -6
0 0 0 0 0 0 0 0	0 0 0 0 0 0 0 0
0 0 0 0 0 0 0 0	0 0 0 0 0 0 0 0
0 0 0 0 0 0 0 0	0 0 0 0 0 0 0 0
0 0 0 0 0 0 0 0	0 0 0 0 0 0 0 0
0 0 0 0 0 0 0 0	0 0 0 0 0 0 0 0
0 0 0 0 0 0 0 0	0 0 0 0 0 0 0 0
-7 1 1 1 1 1 1 1	0 0 0 0 0 0 0 0

0 0 0 0 0 0 0 0	-7 1 1 1 1 1 1 1
0 0 0 0 0 0 0 0	0 0 0 0 0 0 0 0
0 0 0 0 0 0 0 0	0 0 0 0 0 0 0 0
0 0 0 0 0 0 0 0	0 0 0 0 0 0 0 0
0 0 0 0 0 0 0 0	0 0 0 0 0 0 0 0
0 0 0 0 0 0 0 0	0 0 0 0 0 0 0 0
0 0 0 0 0 0 0 0	0 0 0 0 0 0 0 0
0 0 0 0 0 0 0 0	0 0 0 0 0 0 0 0
-6 1 1 1 1 1 1 1	0 0 0 0 0 0 0 0
0 0 0 0 0 0 0 0	-6 1 1 1 1 1 1 1

**Figure 8: first 16 columns and 18 rows of 64x64Kekre Wavelet Transform Matrix**

**3.2.5 Discret Wavelet Transform (DWT)**

The two dimensional Discret Wavelet Transform is applied on the preprocessed image to get features. DWT is based on sub band coding. The discretized image in time domain is analyzed by successive low pass and high pass filters to obtain the DWT

The Haar wavelet which is an orthogonal wavelet is used in our method. It is discontinuous and resembles a step function. It is expressed by the following expressions.

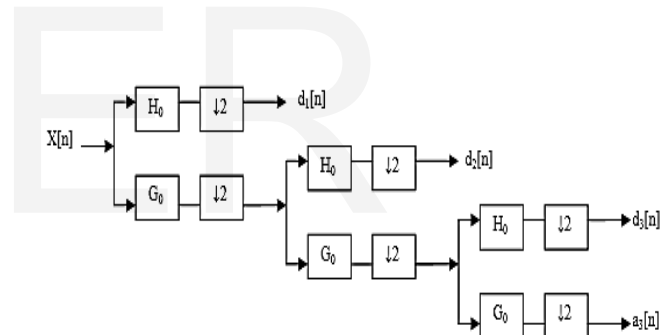


**Figure 9: Three level wavelet decomposition**

$$\psi(x) = \begin{cases} +1 & 0 \leq x \leq 1/2 \\ -1 & 1/2 \leq x \leq 1 \\ 0 & \text{otherwise} \end{cases} \dots\dots\dots (12)$$

$$\phi(x) = \begin{cases} 1 & 0 \leq x \leq 1 \\ 0 & \text{otherwise} \end{cases} \dots\dots\dots (13)$$

One level Haar wavelet is applied to each row and subsequently to the columns of the resulting image. This results in four sub bands, L L, H L, L H, and H H. The L L sub band contains the approximation of the palm image. The other

sub bands contain the edge details. The features are obtained from LL sub band discarding the other detailed bands.

**3.2.6 Euclidean Distance:**

Matching between the data base and test image is done by measuring the distance in vector space or Euclidean space. Perfect match is obtained when this distance is zero. Practically perfect match is never obtained , therefore a threshold is set by trial and error. Thus if the distance is less than the threshold it is taken as a match else a mismatch. The Euclidean Distance is calculated using the equation 14.

$$D(p, q) = \sqrt{(p_i - q_i)^2 + (p_j - q_j)^2} \dots\dots\dots (14)$$

Where  $p_i, p_j$  are features of database and  $q_i, q_j$  are features of test image. The Euclidean distance is applied separately on the KWT and DWT features of the test and database images to obtain the match and mismatch counts from which the FAR and FRR are found.

**3.2.7 EER and TSR**

The EER and TSR of KWT and DWT are found by plotting the FAR and FRR with respect to different values of threshold.

**3.2.8 Fusion**

The fusion at score level is providing excellent results. The EER of the fusion is computed using equation 15.

$$FEER = \left| \frac{\log(EER1)}{\log_2(EER^3)} - \frac{\log(EER2)}{\log_2(EER^3)} \right| \dots\dots\dots (15)$$

EER1=Equal Error Rate for KWT  
EER2=Equal Error Rate for DWT  
TSR of the fusion is found by the formula.

TSR1=Total Success Rate for KWT  
TSR2=Total Success Rate for DWT

**4. ALGORITHM:**

Problem definition: - Authentication of a person based on-palmprint identification using KWT, DWT and fusing of KWT and DWT score levels at matching stage.

**The objectives are**

- To increase Total Success rate (TSR)
- To reduce False Rejection Rate (FRR)
- To reduce False Acceptance Rate (FRR)
- To reduce Equal Error Rate (EER)

The proposed algorithm is given in table 1.

Table1: Proposed palmprint identification algorithm

**Input:** palmprint database ,test palmprint  
**Output:** test palmprint identification

1. The Poly U database is considered, and a database is created to test the proposed algorithm
2. The normalization, segmentation and histogram equalization are used on palmprint image in preprocessing stage.
3. KWT and DWT are applied on preprocessed image to generate KWT and four subbands of DWT.
4. The KWT and approximation band coefficients of DWT are considered as features.
5. The KWT features of test and database images are compared using ED, to compute EER and TSR.
6. The DWT features of test and database palmprint images are compared using ED to compute EER and TSR.
7. The values of EER obtained from KWT and DWT are fused using log transformation.
8.
 
$$FEER = \left| \frac{\log(EER1)}{\log_2(EER^3)} - \frac{\log(EER2)}{\log_2(EER^3)} \right|$$

EER1=Equal Error Rate for KWT  
EER2=Equal Error rate for DWT
9. The values of TSR of KWT and DWT are fused using log transformation
 
$$FTSR = 1 - \left| \frac{\log(TSR1)}{\log_2(TSR^3)} - \frac{\log(TSR2)}{\log_2(TSR^3)} \right|$$

TSR1=total success rate for KWT  
TSR2=total success rate for DWT

**5 PERFORMANCE ANALYSES:**

The Poly U Database is used for performance analysis. The database is created by varying 20 to 100 persons inside database (PID) and persons outside database (POD).

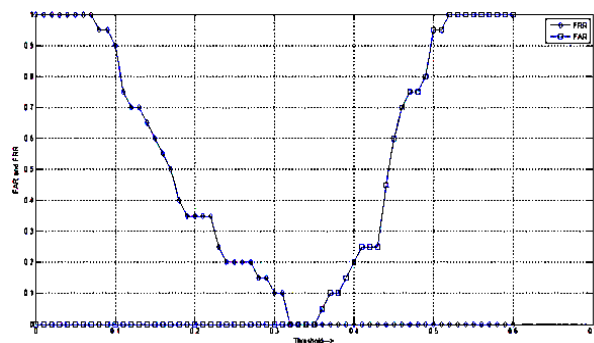


Figure10: Plot of FAR and FRR V/S threshold for KWT

The variations of FRR and FAR with threshold values for KWT with PID: POD is 20:100 are plotted in figure 10. As threshold increases FRR decreases, whereas FAR increases. It is observed that, the value of EER is 0.009 at 0.33 threshold value. The variations of FRR and FAR with threshold values for DWT with PID: POD is 20:100 are plotted in figure 11. As threshold increases FRR decreases, whereas FAR increases. It is observed that, the value of EER is 0.1 at 0.46 threshold value.

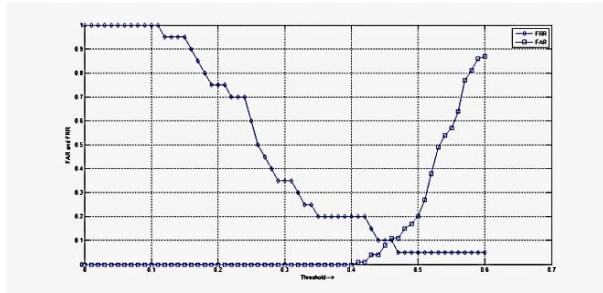


Figure 11: Plot of FAR and FRR V/S threshold for DWT

Table 2: The Variations of EER for DWT, KWT and Proposed Model.

PID	POD	EER (KWT)	EER (DWT)	EER (Proposed Model)
20	100	0.0090	<b>0.100</b>	<b>0.0769</b>
40	80	<b>0.0420</b>	<b>0.1000</b>	<b>0.0412</b>
60	60	<b>0.0550</b>	<b>0.1167</b>	<b>0.0418</b>
80	40	<b>0.0750</b>	<b>0.1000</b>	<b>0.0167</b>
100	20	<b>0.0750</b>	<b>0.1000</b>	<b>0.0167</b>

The variations of EER for KWT, DWT and proposed model are tabulated in Table 2 with variations of PID from 20 to 100 and POD variations from 100 to 20. The values of EER with KWT are lower than DWT. The proposed model has better EER values compared to KWT and DWT.

Table 3: The Variations of TSR for DWT, KWT and Proposed Model.

PID	POD	TSR (KWT)	TSR (DWT)	TSR (Proposed Model)
20	100	<b>99.100</b>	<b>90.000</b>	<b>0.9984</b>
40	80	<b>95.8000</b>	<b>90.0000</b>	<b>0.9989</b>
60	60	<b>94.500</b>	<b>88.300</b>	<b>0.9989</b>
80	40	<b>92.5000</b>	<b>90.0000</b>	<b>0.9995</b>
100	20	<b>92.5000</b>	<b>90.0000</b>	<b>0.9995</b>

Table 4: Comparison of proposed model TSR values with existing algorithms.

Author & Reference	Feature Extraction	Matching	% TSR
H B Kekre, et al. [21]	KWT	Euclidean Distance and relative Energy entropy.	85.63
Haifeng Sang et al.[22]	Local Binary Pattern (LBP)	Chi- Square Statistics	97.012
Jingyuguo et al [23]	Entropy Map and 2DPCA.	Nearest neighbor Classification	79.6
AB khalifa.[24]	DWT, Gabor Filter & Co-Occurrence Matrix	SVM. Best results by DWT.	95.2
Proposed	fusion of KWT and DWT	Euclidean Distance	99.95

The percentage TSR values of proposed algorithm are compared with existing algorithms are given in table 4. The percentage value of TSR is high in the case of proposed algorithm compared to existing algorithms such as Kekre et al., [22]. Haifeng sang et al., Kalifa [4] and linzhang et al.,[16]. The performance of proposed algorithm is better compared to existing algorithms, since the performance parameters are fused using log transformation at the matching stage.

**6. CONCLUSION**

In this paper, PIFKDM algorithm is proposed. The palmprint images are preprocessed to generate ROI palmprint. The features are extracted using KWT and DWT. The ED is used to compare features of test image with database images. The values of EER and TSR are computed using KWT and DWT techniques. The values of EER and TSR obtained from KWT and DWT are fused using Log transformation to enhance performance. It is observed that the values of EER and TSR are better in the case of proposed algorithm. In future, the DWT can be replaced by Dual Tree complex wavelet Transform.

**ACKNOWLEDGMENT**

We thank the HOD, Principal and management of DayanandaSagar College of Engineering, and Rayalseema University for their support in accomplishing this work.

**REFERENCES**

[1] H B Kekre, Tanuja Sarode, Rekha Vij, "Multi Resolution Analysis of Multi Spectral Palmprints using Hybrid Wavelets for Identification", *International Journal of Advanced*

- Computer Science and Applications*, VOL 4, PP 192-198, 2013.
- [2] Xingpeng Xu, Zhenhua Guo, Changjiang Song, Yafeng Li, "Multispectral Palmprint recognition using Quaternion Matrix", *Sensors*, PP 4633-4647, 2012.
- [3] Wei Li, Lei Zhang, David Zhang, Guangming Lu, Jingqi Yan, "Efficient Joint 2D and 3D Palmprint Matching with Alignment Refinement", *IEEE Conference on vision and pattern recognition*, PP 795- 801, 2010.
- [4] Wei lei, Zhang B, Lei Zhang, Jing quid Yan, "Principle Line Based Alignment Refinement for Palm print R recognition", *IEEE Transactions on Systems, Man and Cybernetics*, Vol 42, PP 1491-1499, 2012.
- [5] Kumar A, Hanmandalu M, Madasu VA, Vasikarla.S, "A Palmprint Authentication System using Quantized Phased Feature Representation", *IEEE Workshop on Applied Imagery Pattern Recognition (AIPR)* PP 1-8, 2011.
- [6] Ruiqiong shi, Dongmei Sun, "A New Security Scheme Based on Palmprint Biometrics for Signature", *IEEE International Conference on Biometrics: Theory, Applications and systems*, PP1-6, 2007.
- [7] Eryun Liu, Anil K Jain, Jie Tian, "A Course to Fine Minutiae Based Latent Palmprint Matching", *IEEE Transactions on Pattern Analysis and Machine Intelligence*, 2013.
- [8] Feng Yue, Bin Li, Ming Yu, and Jiaqiang Wang, "Hashing Based Fast Palmprint Identification for Large Scale Data Bases", *IEEE Transactions on Information, Forensics and Security*, Vol 8, 2012.
- [9] V Struc and N Pavesic, "A Comparison of Feature Normalization Techniques for PCA based Palmprint Recognition", *International Conference, MATHMOD, Vienna, Austria*, PP 2450-2453, 2009.
- [10] Lin Lin Shen, Shipei Wu, Songhao Zheng and Zhen Ji, "Embedded Palmprint Recognition System using OMAP 3530", *Sensors*, PP 1482-1493, 2012.
- [11] Gandehari A, and Avanthipur M, "Palmprint Verification and Identification using Pyramidal HOG Features and Fast Tree based Matching", *Fifth IAPR International Conference on Biometrics*, PP 421-426, 2012.
- [12] K W Chau, "Palmprint Identification using Restricted Fusion", *Journal of Applied Mathematics and Computation, Elsevier*, PP 927-924, 2008.
- [13] R Gayathri and R Ramamurthi, "Multifeature Palmprint Recognition using Feature Level Fusion", *International Journal of Engineering and Research Applications*, Vol.2, PP 1048-1054. 2012.
- [14] Lin Zhang, Hang Yu Li and Jun Yu Nin, "Fragile bits in Palmprint Recognition", *IEEE Signal Processing Letters*, Vol 19, PP 663-666, 2012.
- [15] Dakshina R K, Ajitha R, Phalguni G, Jamuna K S, Jinson Hwang, "Human Identity Verification using Multispectral Palmprint Fusion", *Journal of Signal and Information Processing, Scientific Research*, PP 263-273, 2012.
- [16] Hanmandalu M, Neha Mittal, Ankit G, Ritu V, "A Comprehensive Study of Palmprint based Authentication", *International Journal of Computer Applications*, Vol.2, PP 1048 – 1054, 2012.
- [17] Capelli R, Ferrara M, Maio D, "A fast and accurate palmprint system based on minutiae", *IEEE Transactions on Systems, Man, and cybernetics*, Vol 42, PP 956-962, 2012.
- [18] Huan Zhang, "A Fast Palmprint Recognition Verification System based on Fractal Coding", *International Journal of Information Acquisition*, Vol 9, Issue 1, 2013.
- [19] Dr. Vinayak Ashok Baradi, "Texture Feature Extraction For Biometric Authentication using Partitioned Complex Planes in Transform Domain", *International Conference & Workshop on Emerging Trends in Technology*, PP 39 -45, 2012.
- [20] Dr. Kekre, Archana, Athavale and Dipali Sadavarthi, "Algorithm to Generate Kekre's Wavelet Transform from Kekre's Transform", *International Journal of Engineering Science and Technology*, Vol.2, PP 756-767, 2010.
- [21] H B Kekre, V A Baradi, V I Singh, A A Ambedkar, "Palmprint Recognition Using Kekre's Wavelet's Energy Entropy Based Feature Extraction", *International Conference & Workshop on Emerging Trends in Technology*, PP 39 -45, 2011.
- [22] Haifeng Sang, Yueshi Ma, Jing Huang, "Robust Palmprint Recognition Based on Touch less Color Palmprint Images Acquired", *Scientific Research, journal of Signal and Information Processing*, Vol 4, PP 134-139, 2013.
- [23] Jingyuguo, Yuqin Liu, Weiqi Yuan, Dan Long, "Palmprint Recognition using Entropy Map and 2DPCA from a Single image per Person", *Journal of Computational Information Systems*, PP 3415-3421, 2013.